NANO LETTERS

2001
Vol. 1, No. 1
3−7

Letters

High-Quality Manganese-Doped ZnSe Nanocrystals

D. J. Norris*

NEC Research Institute, 4 Independence Way, Princeton, New Jersey 08540

Nan Yao

Princeton Materials Institute, Princeton University, 70 Prospect Avenue, Princeton, New Jersey 08540

F. T. Charnock and T. A. Kennedy

Naval Research Laboratory, Washington, D.C. 20375

Received August 2, 2000

ABSTRACT

We demonstrate high-quality, highly fluorescent, ZnSe colloidal nanocrystals (or quantum dots) that are doped with paramagnetic Mn^{2+} impurities. We present luminescence, magnetic circular dichroism (MCD), and electron paramagnetic resonance (EPR) measurements to confirm that the Mn impurities are embedded inside the nanocrystal. Optical measurements show that by exciting the nanocrystal, efficient emission from Mn is obtained, with a quantum yield of 22% at 295 K and 75% below 50 K (relative to Stilbene 420). MCD spectra reveal an experimental Zeeman splitting in the first excited state that is large (28 meV at 2.5 T), depends on doping concentration, and saturates at modest fields. In the low field limit, the magnitude of the effective *g* factor is 430 times larger than in undoped nanocrystals. EPR experiments exhibit a six-line spectrum with a hyperfine splitting of 60.4×10^{-4} cm^{-1}, consistent with Mn substituted at Zn sites in the cubic ZnSe lattice.

Nanometer-scale semiconductor crystallites, also referred to as nanocrystals or quantum dots, have been extensively studied to explore their unique properties and potential applications.[1] Interesting behavior arises in these materials due to the confinement of optically excited electron−hole pairs by the crystallite boundary. However, while the basic explanation of this phenomenon, known as the quantum size effect, was provided early in the investigation of these materials,[2−4] a detailed understanding required the advent of high-quality colloidal nanocrystals, which were uniform in size, shape, crystallinity, and surface passivation. Once such materials became available,[5] tremendous progress was made in a variety of physical studies. Consequently, many of the properties of semiconductor nanocrystals are now understood in detail.[1] In addition, high-quality crystallites have led to more complicated nanocrystal-based structures, such as quantum-dot solids,[6] light-emitting devices,[7] and even photonic crystals.[8]

These successes have encouraged researchers to go beyond pure nanocrystals and investigate particles that are intention-

* E-mail address: dnorris@research.nj.nec.com.
Homepage: www.neci.nj.nec.com/homepages/dnorris/.

10.1021/nl005503h CCC: $20.00
Published on Web 11/28/2000

Report Documentation Page

Form Approved
OMB No. 0704-0188

1. REPORT DATE	2. REPORT TYPE	3. DATES COVERED
02 AUG 2000		**00-00-2000 to 00-00-2000**

4. TITLE AND SUBTITLE	5a. CONTRACT NUMBER
High-Quality Manganese-Doped ZnSe Nanocrystals	5b. GRANT NUMBER
	5c. PROGRAM ELEMENT NUMBER
6. AUTHOR(S)	5d. PROJECT NUMBER
	5e. TASK NUMBER
	5f. WORK UNIT NUMBER
7. PERFORMING ORGANIZATION NAME(S) AND ADDRESS(ES) **Naval Research Laboratory,Washington,DC,20375**	8. PERFORMING ORGANIZATION REPORT NUMBER
9. SPONSORING/MONITORING AGENCY NAME(S) AND ADDRESS(ES)	10. SPONSOR/MONITOR'S ACRONYM(S)
	11. SPONSOR/MONITOR'S REPORT NUMBER(S)

12. DISTRIBUTION/AVAILABILITY STATEMENT
Approved for public release; distribution unlimited

13. SUPPLEMENTARY NOTES

14. ABSTRACT
see report

15. SUBJECT TERMS

16. SECURITY CLASSIFICATION OF:			17. LIMITATION OF ABSTRACT	18. NUMBER OF PAGES	19a. NAME OF RESPONSIBLE PERSON
a. REPORT **unclassified**	b. ABSTRACT **unclassified**	c. THIS PAGE **unclassified**	**Same as Report (SAR)**	**5**	

ally doped with impurities. Much effort has focused on II−VI semiconductor nanocrystals, such as ZnS or CdS, which are doped with Mn.[9−15] Ideally, Mn^{2+} acts as a paramagnetic center ($S = {}^5/_2$) which substitutes for the group II cation in the semiconductor lattice. Initially, this choice was motivated by the analogous bulk materials, referred to as dilute magnetic semiconductors (DMS). Because of the sp−d exchange interaction between the semiconductor and the Mn, bulk DMS crystals have interesting magnetic and magnetooptical properties.[16] DMS nanocrystals should exhibit even more exotic behavior since spin−spin exchange interactions should be enhanced by the confinement of the electron and hole.[15] However, more recently, an additional motivation was recognized. DMS nanocrystals can be used to study and manipulate a single spin (or small number of spins) that is trapped in a semiconductor quantum box.[17] In addition to interesting physics, this possibility implies that DMS quantum dots can provide a useful model system for the new field of *spintronics*.[18]

Unfortunately, to date, all doped crystallites have been of much lower quality than the best pure materials. This has limited our ability to study DMS nanocrystals and find applications for their unique properties. If better samples were available, this situation could change dramatically. To obtain high-quality DMS nanocrystals, an obvious approach is to use a high-temperature (>300 °C) chemical reaction similar to that used for the best undoped samples.[5] The reaction would then provide sufficient thermal energy to anneal out defects in the nanocrystal. However, since any embedded impurity atom would always be within a few lattice constants of the surface of the nanocrystal, the same thermal energy can anneal out the Mn "defect". This possibility, that high-temperature reactions eliminate Mn from the nanocrystal, has recently gained acceptance due to two findings: (1) room temperature reactions can easily produce low-quality, Mn-doped, nanocrystals and (2) extensive efforts to make high-quality, Mn-doped, CdSe nanocrystals using the high-temperature approach found that Mn segregated to the particle surface.[14] The discouraging implication of these results is that Mn doping is incompatible with the preparation of high-quality nanocrystals.

However, in this Letter, we show that this conclusion is incorrect. We prepare ZnSe:Mn nanocrystals, made via a high-temperature reaction, that are not only superior to previously doped II−VI materials but are also comparable in quality to the best undoped particles. Since Mn was shown to segregate to the surface of similarly prepared CdSe nanocrystals,[14] we must prove that Mn is actually embedded inside our particles. We provide optical, magnetic circular dichroism (MCD), and electron paramagnetic resonance (EPR) evidence for support.

Our ZnSe nanocrystals were prepared by using the high-temperature, organometallic synthesis of Hines et al.[19] This procedure, which leads to highly crystalline, zinc blende, ZnSe nanocrystals that exhibit extremely efficient luminescence, was adapted to Mn doping. Although diethylmanganese has been used previously as an organometallic source for Mn,[10] here we used dimethylmanganese ($MnMe_2$). While both dialkylmanganese species are metastable, the lifetime of $MnMe_2$ is significantly longer.[20] In a typical procedure, $MnMe_2$ was freshly prepared in a helium glovebox by reacting 0.5 mL of a 0.2 M $MnCl_2$ slurry in anhydrous tetrahydrofuran (THF) with 0.2 mL of 3 M methylmagnesium chloride in THF. (Unless noted, all chemicals were purchased from Aldrich and used without purification.) The resulting clear golden solution was then diluted with 1.8 mL of anhydrous toluene. Subsequently, 0.5 mL of this 0.04 M $MnMe_2$ solution (0.02 mmol) was added to a syringe containing 4 mL of trioctylphosphine (TOP, Fluka), 1 mL of 1 M Se in TOP (Alfa Aesar), and 82 μL of diethylzinc (Strem, 0.8 mmol). The syringe was removed from the glovebox and rapidly injected into a vigorously stirred reaction vessel with 15 mL of distilled HDA at 310 °C under dry nitrogen. The absorption spectrum of a small aliquot, removed immediately after injection, typically revealed an absorption feature around 320 nm, characteristic of small ZnSe nanocrystals.[19] These nanocrystals were then grown at 240−300 °C. Once the final desired size was obtained, as monitored by absorption, the particles were isolated from the growth solution using standard methods[5,19] and stored under an inert atmosphere. The properties reported below were observed even after samples were a year old. The final concentration of Mn was adjusted by changing the amount of $MnMe_2$ added to the reaction. Below, we designate the samples by their initial Mn:Zn concentration in atomic percent, C_I. However, a much lower percentage of the Mn is actually incorporated into the nanocrystals, as discussed below.

Figure 1 shows absorption spectra for a small size series of nanocrystals, both doped and undoped, which demonstrate the quality of our samples. Because of the quantum size effect, a series of electronic transitions appear, which are shifted to higher energy than the bulk band gap ($E_g = 2.58$ eV). Such spectra were acquired after size-selective precipitation[5] was used to further narrow the size distribution and improve the original ZnSe procedure.[19] Since the second excited state can be clearly resolved (e.g., see sample E in Figure 1), the spectra appear strikingly similar (at least qualitatively) to the best CdSe spectra.[5] Measurements of the size distribution by transmission electron microscopy (TEM) suggest that the standard deviation in size is 6%. However, due to measurement error caused by low Z-contrast in ZnSe, this value is only an upper bound.

The first evidence indicating successful doping was obtained from luminescence. Unlike many nanocrystal systems that do not emit at all or emit weakly from red-shifted trap states, ZnSe crystallites exhibit efficient emission.[19] Figure 2a shows photoluminescence (PL) and photoluminescence excitation (PLE) spectra for an undoped sample (sample F in Figure 1). In PL, strong blue emission (from the lowest excited electron−hole pair state) was observed when the sample was excited with 350 nm light; no red-shifted emission was present. In PLE, a narrow spectral band of this blue emission was monitored while scanning the excitation energy. The resulting spectrum in Figure 2a shows a series of absorption features that lead to

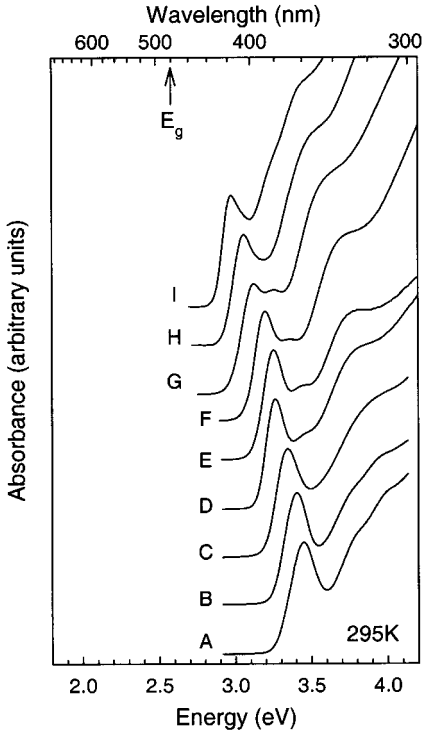

Figure 1. Absorption spectra for a size series of ZnSe nanocrystals at 295 K. Mean diameters, D, and initial Mn concentrations, C_I: (A) <27 Å, 0%; (B) <27 Å, 0%; (C) 27 Å, 0%; (D) 27.5 Å, 0.5%; (E) 28.0 Å, 0%; (F) 30.5 Å, 0%; (G) 36.0 Å, 2.5%; (H) 43.0 Å, 2.5%; (I) 57.5 Å, 2.5%. The sizes are estimated from the first absorption maxima by using previous TEM measurements on undoped ZnSe nanocrystals.[19,21] The energy of the bulk band gap, E_g, for ZnSe is shown (↑).

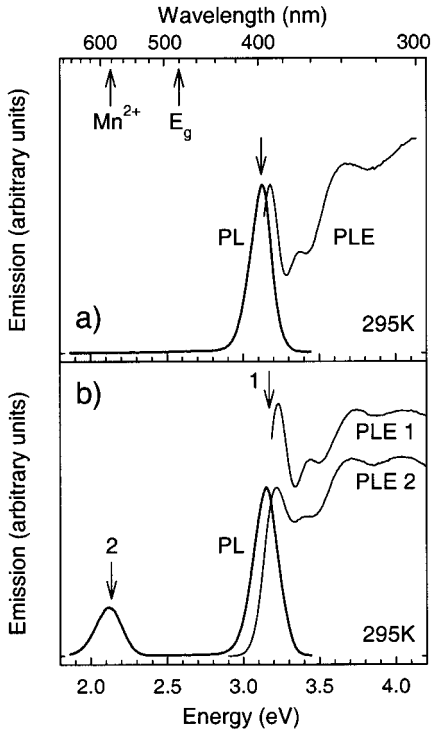

Figure 2. Photoluminescence (PL) and photoluminescence excitation (PLE) spectra at 295 K. (a) An undoped sample (F in Figure 1). In PL, excitation is at 3.542 eV (350 nm). In PLE, the monitored emission is at 3.123 eV (↓). The energy of E_g and Mn emission in bulk ZnSe are shown (↑). (b) A doped sample (D = 28.5 Å, C_I = 3.1%). In PLE1, the band edge emission was monitored at 3.171 eV (1↓). In PLE2, the Mn emission was monitored at 2.138 eV (2↑). Because of size selection, the features in PLE1 are better resolved than in PLE2. No size selection was ever observed by monitoring different positions on the Mn^{2+} emission.

the blue emission. These features are consistent with the absorption of ZnSe nanocrystals, as shown in Figure 1. In contrast to the above, the PL spectra of doped samples (see Figure 2b) show an additional red-shifted emission feature with a maximum at 2.12 eV (585 nm). Since similar red emission is observed in bulk ZnSe:Mn at 2.13 eV and is assigned to an internal Mn^{2+} transition ($^4T_1 \rightarrow {}^6A_1$),[22] our 2.12 eV line is consistent with Mn emission. Furthermore, a comparison of PLE spectra obtained by monitoring the blue emission (PLE1 in Figure 2b) with that obtained by monitoring the Mn emission (PLE2 in Figure 2b) shows that the same ZnSe absorption features are responsible for both. Thus, the PLE results indicate, as suggested for other materials,[9,10] that energy transfer from the photoexcited ZnSe nanocrystal to the Mn gives rise to the red emission.

The strength of this emission depends on the Mn concentration. Figure 3a shows how the Mn emission changes during growth for a sample with C_I = 2.5%. As the blue emission shifts to lower energy (i.e., the particles get larger), the Mn feature grows in intensity. This is consistent with an increase in the average number of Mn per nanocrystal during growth. This can occur either through Ostwald ripening[5] or by incorporation of excess Mn from the growth solution. In either case, comparable emission intensity should be observed in smaller sizes by increasing C_I. This is verified in Figure 3b where strong Mn emission is observed in a 28.5 Å sample with C_I = 6.3%. For this sample, the Mn emission quantum yield (Y_Q) is 22% at room temperature and 75% at temperatures less than 50 K (Figure 3c). Thus, the energy transfer from the ZnSe nanocrystal to the Mn impurity is extremely efficient in these samples.

However, while evidence of energy transfer is compelling data in favor of successful doping, it does not guarantee that Mn has substituted for Zn in the nanocrystal. Energy transfer could potentially occur if Mn were on the surface of the nanocrystal or in the surrounding matrix.[14] Thus, to test this possibility, several additional experiments were performed to confirm that Mn is inside the lattice. First, repeated cap exchanges with pyridine, which can remove Mn from the surface of CdSe nanocrystals,[14] did not alter any of the above optical results. When our pyridine-capped ZnSe nanocrystals were redispersed in hexane with a small amount of TOP and TOPO, the strong Mn emission returned.

Second, EPR experiments on our samples are consistent with Mn embedded inside the nanocrystal. We obtain six-line spectra, as in Figure 4a, which arise due to the hyperfine interaction with the ^{55}Mn nuclear spin ($I = {}^5/_2$). Since the hyperfine splitting is strongly dependent on the local environment, EPR spectra can be used to determine the location of the Mn.[23] From Figure 4a, we extract a hyperfine splitting of 60.4×10^{-4} cm^{-1}. This value agrees well with that obtained for Mn at cubic lattice sites in bulk ZnSe (61.7

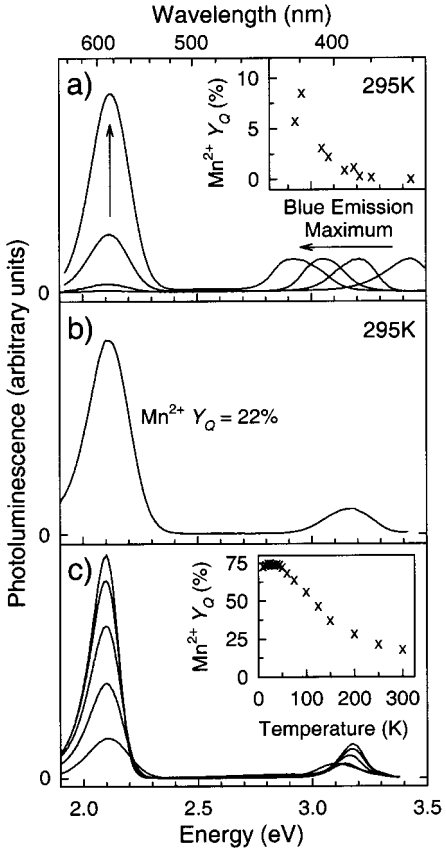

Figure 3. (a) PL vs growth at 295 K for a sample with $C_I = 2.5\%$. Aliquots are removed from the growth solution and diluted with hexane. As the blue emission of the nanocrystal shifts to lower energy, the Mn emission increases in intensity. The spectra, which represent samples with diameters <27, 28, 40, and 63 Å, are normalized to the intensity of the blue feature. The inset shows the Mn emission quantum yield (Y_Q), relative to Stilbene 420 laser dye, vs the blue emission maximum. (b) PL at 295 K for a sample with $D = 28.5$ Å, $C_I = 6.3\%$. The sample was isolated three times by size-selective precipitation and then redissolved in hexane with a small amount of trioctylphosphine and TOPO. After this treatment, Y_Q of Mn is 22%. (c) PL vs temperature for the sample from (b). The inset shows that Y_Q for Mn increases to 75% below 50 K.

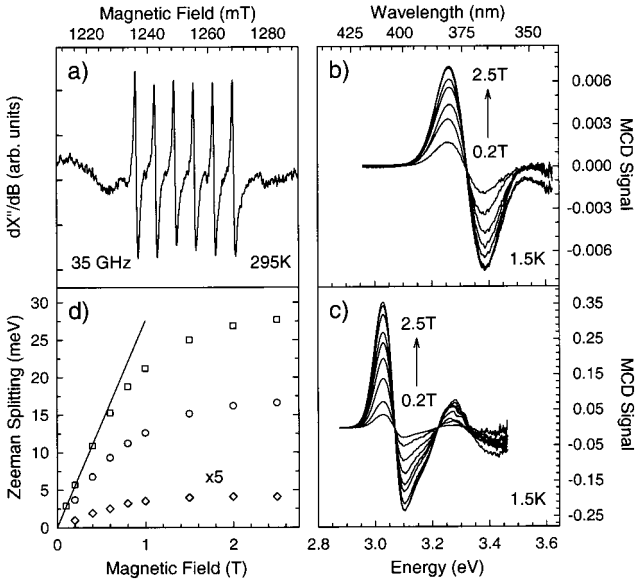

Figure 4. (a) EPR spectrum taken at 35 GHz and 295 K in a Varian E109Q spectrometer for a sample with $D = 29.0$ Å; $C_I = 1.0\%$. (b) and (c) MCD spectra vs magnetic field from 0.2 to 2.5 T at 1.5 K. The MCD signal, $[I^+(E) - I^-(E)]/[I^+(E) + I^-(E)]$, is normalized by the optical density at the maximum of the lowest absorption feature. It is measured in the Faraday geometry using a photoelastic modulator and a lock-in amplifier. The sign of the signal was determined. (b) and (c) show data for samples with $D = 29.0$ Å, $C_I = 1.0\%$ and $D = 53.0$ Å, $C_I = 2.5\%$, respectively. (d) The Zeeman splitting (ΔE) vs magnetic field extracted using ref 28 from the data in (b) (diamonds) and (c) (squares). Data for an additional sample, $D = 42.0$ Å, $C_I = 2.5\%$, is also shown (circles). (b) is scaled by 5. The solid line shows a linear fit to the data from (c) in the low field limit. From the slope we obtain $g_{eff} = 475$.

$\times 10^{-4}$ cm^{-1}).[24] Thus, we conclude that the majority of the Mn is substituted for Zn in the nanocrystal. Although signals from lower symmetry sites (e.g., at or near the surface) are also present in our samples, it is much smaller. In contrast, the EPR spectra from many previous samples were dominated by these lower symmetry signals. In fact, it was this observation that initially suggested that Mn-doping of CdSe was problematic.

Third, we obtain MCD results (Figure 4) that can only be explained by internal Mn. In general, MCD can probe the influence of an external magnetic field on the position of an absorption feature.[15,25−27] Typically, the field causes the absorption maxima for right (E^+) and left (E^-) circularly polarized light to be shifted to higher and lower energy, respectively. The goal of the MCD experiment is to extract the Zeeman splitting, $\Delta E = E^+ - E^-$. This can be achieved by measuring the quantity $[I^+(E) - I^-(E)]/[I^+(E) + I^-(E)]$, where $I^+(E)$ and $I^-(E)$ are the energy-dependent transmitted intensities of right and left circularly polarized beams.[15] If ΔE is small compared to the absorption line width, Γ, the MCD signal is well approximated by the derivative of the absorption line shape. ΔE can then easily be obtained from the magnitude of the MCD signal.[28]

Previously, MCD has been used on undoped nanocrystals to extract ΔE and obtain information about how the spin sublevels of the lowest electron−hole pair state move with external field.[25−27] Here, however, the MCD technique is used for a slightly different purpose. In Mn-doped nanocrystals, the electron−hole pair can be strongly influenced by the effective magnetic field caused by the Mn spin.[15] Since this effect requires wave function overlap between the confined electron−hole pair and the Mn, it occurs only for Mn *inside* the nanocrystal. In this case, the field, which is independent from and much larger than any externally applied field, causes a giant spin sublevel splitting *even at zero applied field*. Unfortunately, this splitting cannot be observed on an ensemble of nanocrystals at zero field since the Mn spins are randomly oriented. However, if we use a modest external field to partially align the Mn spins, the MCD spectrum will reveal this splitting. In other words, we combine an external field and MCD to reveal, *not cause*, the splitting. At higher applied fields, when all of the Mn are completely aligned, the magnitude of the MCD signal should saturate. Thus, strong evidence for internal Mn can be obtained if we observe large MCD signals that saturate at modest fields.

This behavior is clearly observed in Figure 4. From our MCD spectra, we extracted the field dependence of the Zeeman splitting for three of our doped samples and an undoped control sample. While the control sample exhibited a small Zeeman splitting ($\Delta E = -0.16$ meV at 2 T) that increased linearly with field, in Figure 4d our doped samples show, as expected, a splitting that is more than 2 orders of magnitude larger (as large as 28 meV at 2.5 T), depends on doping concentration, and saturates at modest fields. Similar behavior was recently observed in CdS:Mn nanocrystals and used as strong evidence for internal Mn and the giant internal magnetic field.[15] Here, we observe a splitting that is $\sim 10\times$ larger. In terms of an effective g factor, g_{eff},[27] the sample in Figure 4c exhibits a g_{eff} of 475 in the small field limit (see line in Figure 4d). In comparison, the control sample has a g_{eff} of -1.1. From these values we can estimate that the presence of the Mn inside the nanocrystal induces an effective internal magnetic field of ~ 430 T. While this value is impressive, we note that theory predicts that the internal field should be even larger in a perfect sample, but inhomogeneities in the number and position of Mn within the nanocrystal cause the average effect to decrease.[15] Nevertheless, at 28 meV, the Zeeman splitting, which we emphasize should be present even at zero applied field, is comparable to kT at room temperature (25 meV).

In addition to providing evidence for successful doping, our MCD data also provide clues about the concentration of Mn in our samples. The MCD signal, which increases with C_{I}, suggests that our nanocrystals are in the limit of 1 Mn per crystallite or less. If, instead, they were above this limit, an increase in C_{I} would lead to Mn−Mn interactions that would reduce the internal magnetic field and the resulting MCD signal.[15] The limit of 1 Mn per crystallite implies that the final concentration of Mn in the nanocrystal is 1−5% of C_{I}, i.e., an atomic Mn:Zn ratio of 0.025−0.125%. This conclusion is also consistent with energy-dispersive X-ray measurements on pyridine-exchanged (6x) samples. We detect trace Mn that is below our sensitivity for quantitative analysis (Mn:Zn < 0.3%).

An interesting question that remains is whether a single Mn-doped nanocrystal can emit from both the lowest electron−hole pair state and the internal Mn transition. As seen in Figure 3, a small amount of blue emission remains even in samples with strong Mn fluorescence. This would occur if direct electron−hole recombination were competitive with the energy transfer process. In this case, a single Mn-doped nanocrystal could emit from both lines. On the other hand, another explanation, which we feel is more likely, is that these two features arise separately from undoped and doped quantum dots in the sample. In the limit of one Mn per crystallite or less, some crystallites in the distribution will remain undoped and give rise to blue emission. This explanation is supported by preliminary data in which the blue emission disappears completely at even higher Mn concentration. However, further study is required to resolve this issue definitively.

In summary, we have demonstrated a simple method to prepare high-quality ZnSe nanocrystals that are doped with Mn impurities. This method leads to nearly monodisperse, highly fluorescent, crystalline quantum dots that can be systematically prepared as a function of size. Optical, MCD, and EPR measurements all confirm that the Mn impurity is embedded inside the nanocrystal in the limit of one per nanocrystal (or less). Furthermore, preliminary results suggest that samples at higher Mn concentrations may also be achievable by this method. Therefore, this system should provide a model material for gaining a detailed understanding of DMS nanocrystals and their potential applications.

Acknowledgment. We thank M. Bawendi, Al. Efros, F. Mikulec, C. B. Murray, J. Schwartz, and P. Wolff for helpful discussions and M. Beyer and K. McIlwrath (Hitachi) for assistance. F.T.C. acknowledges support from a NRC-NRL Research Associateship.

References

(1) Alivisatos, A. P. *J. Phys. Chem.* **1996**, *100*, 13226. *Science* **1996**, *271*, 933.
(2) Efros, Al. L.; Efros, A. L. *Sov. Phys. Semicond.* **1982**, *16*, 772.
(3) Ekimov, A. I.; Onushchenko, A. A. *Sov. Phys. Semicond.* **1982**, *16*, 775.
(4) Brus, L. E. *J. Chem. Phys.* **1983**, *79*, 5566.
(5) Murray, C. B.; Norris, D. J.; Bawendi, M. G. *J. Am. Chem. Soc.* **1993**, *115*, 8706.
(6) Murray, C. B.; Kagan, C. R.; Bawendi, M. G. *Science* **1995**, *270*, 1335.
(7) Colvin, V. L.; Schlamp, M. C.; Alivisatos, A. P. *Nature* **1994**, *370*, 354.
(8) Vlasov, Yu. A.; Yao, N.; Norris, D. J. *Adv. Mater.* **1999**, *11*, 165.
(9) Wang, Y.; Herron, N.; Moller, K.; Bein, T. *Solid State Commun.* **1991**, *77*, 33.
(10) Bhargava, R. N.; Gallagher, D.; Hong, X.; Nurmikko, A. *Phys. Rev. Lett.* **1994**, *72*, 416.
(11) Oka, Y.; Yanata, K. *J. Lumin.* **1996**, *70*, 35.
(12) Sooklal, K.; Cullum, B. S.; Angel, S. M.; Murphy, C. J. *J. Phys. Chem.* **1996**, *100*, 4551.
(13) Levy, L.; Hochepied, J. F.; Pileni, M. P. *J. Phys. Chem.* **1996**, *100*, 18322. Levy, L.; Feltin, N.; Ingert, D.; Pileni, M. P. *J. Phys. Chem. B* **1997**, *101*, 9153. Feltin, N.; Levy, L.; Ingert, D.; Vincent, E.; Pileni, M. P. *J. Appl. Phys.* **2000**, *87*, 1415.
(14) Mikulec, F. V.; Kuno, M.; Bennati, M.; Hall, D. A.; Griffin, R. G.; Bawendi, M. G. *J. Am. Chem. Soc.* **2000**, *122*, 2532.
(15) Hoffman, D. M.; Meyer, B. K.; Ekimov, A. I.; Merkulov, I. A.; Efros, Al. L.; Rosen, M.; Couino, G.; Gacoin, T.; Boilot, J. P. *Solid State Commun.* **2000**, *114*, 547.
(16) Furdyna, J. K. *J. Appl. Phys.* **1988**, *64*, R29.
(17) Gupta, J. A.; Awschalom, D. D.; Peng, X.; Alivisatos, A. P. *Phys. Rev. B* **1999**, *59*, R10421.
(18) Awschalom, D. D.; Kikkawa, J. M. *Phys. Today* **1999**, *52*, 33.
(19) Hines, M. A.; Guyot-Sionnest, P. *J. Phys. Chem. B* **1998**, *102*, 3655.
(20) Tamura, M.; Kochi, J. *J. Organomet. Chem.* **1971**, *29*, 111.
(21) Shim, M.; Guyot-Sionnest, P. Personal communication.
(22) Oczkiewicz, B.; Twardowski, A.; Demianiuk, M. *Solid State Commun.* **1987**, *64*, 107. Xue, J.; Ye, Y.; Medina, F.; Martinez, L.; Lopez-Rivera, S. A.; Giriat, W. *J. Lumin.* **1998**, *78*, 173.
(23) Kennedy, T. A.; Glaser, E. R.; Klein, P. B.; Bhargava, R. N. *Phys. Rev. B* **1995**, *52*, R14356.
(24) Ludwig, G. W.; Woodbury, H. H. Electron Spin Resonance in Semiconductors. In *Solid State Physics*; Seitz, F., Turnbull, D., Eds.; Academic Press: New York, 1962; Vol. 13; p 298.
(25) Ando, K.; Yamada, Y.; Shakin, V. A. *Phys. Rev. B* **1993**, *47*, 13462.
(26) Nomura, S.; Misawa, K.; Segawa, Y.; Kobayashi, T. *Phys. Rev. B* **1993**, *47*, 16024. Nomura, S.; Segawa, Y.; Kobayashi, T. *Phys. Rev. B* **1994**, *49*, 13571.
(27) Kuno, M.; Nirmal, M.; Bawendi, M. G.; Efros, Al.; Rosen, M. *J. Chem. Phys.* **1998**, *108*, 4242.
(28) $\Delta E = [4\Gamma I^{\max}]/[\ln(10)\, D^{\max}]$, where $I^{\max}$ is the maximum intensity of the MCD signal and $D^{\max}$ is the optical density of the sample at the $I^{\max}$ energy.

NL005503H